Journal of Electrochemical Science and Technology
Vol. 3, No. 1, 2012, 50-56
http://dx.doi.org/10.5229/JECST.2012.3.1.50

Journal of Electrochemical Science and Technology

A Kinetic Investigation of Ethanol Oxidation on a Nickel Oxyhydroxide Electrode

I. Danaee[a], M. Jafarian[b†], M. Sharafi[b], F. Gobal[c]
[a]*Abadan Faculty of Petroleum Engineering, Petroleum University of Technology, Abadan, Iran*
[b]*Department of chemistry, K. N. Toosi University of Technology, Tehran, Iran*
[c]*Department of chemistry, Sharif University of Technology, Tehran, Iran*

ABSTRACT :

Nickel modified NiOOH electrodes were used for the electrocatalytic oxidation of ethanol in alkaline solutions where the methods of cyclic voltammetry (CV) and chronoamperometry (CA) were employed. In CV studies, in the presence of ethanol, an increase in the current for the oxidation of nickel hydroxide is followed by a decrease in the corresponding cathodic current. This suggests that the oxidation of ethanol is being catalysed through mediated electron transfer across the nickel hydroxide layer comprising of nickel ions of various valence states. Under the CA regime the reaction followed a Cottrellian behavior and the diffusion coefficient of ethanol was found to be 1×10^7 cm^2 s^{-1}.

Keywords: Ethanol, Electrocatalytic, Nickel, Modified electrode

Received March 18, 2012 : Accepted March 28, 2012

1. Introduction

In the past decades, the direct methanol fuel cell (DMFC) has drawn attention for its simple construction with reduced dimensions and high-energy efficiency. Progress has been made in this field.[1-3] However, the intrinsic disadvantage of DMFC is the toxicity of methanol. Therefore, researchers have looked for other small molecule alcohols as alternative fuels.[4,5] Ethanol has emerged as the first choice because of its non-toxicity and low volatility together with a higher energy density than methanol (8.01 kWh kg^{-1} versus 6.09 kWh kg^{-1})[6]. Other important considerations for choosing ethanol are its low price, natural availability, renewability, a higher power density, zero green-house contribution to the atmosphere and its transportability. Among the published reports on proton exchange membrane fuel cells (PEMFC) with alcohol as fuel,[5-9] the direct ethanol fuel cell (DEFC) seems promising, especially for the application in devices like electric vehicles, mobile telephone and laptops. Oxidizable metal Pt and Pt alloy[10-12] electrodes provide simple way for the catalytic oxidation of ethanol.

The main difficulty of ethanol application in fuel cells is still the low current density obtained due to the process of self-poisoning promoted by the strongly adsorbed reaction intermediate species on platinum. These species can be CO or other carbonated species with one or two carbon atoms.[13-19] The main intrinsic problem is the strong interaction of the adsorbed intermediates with the active sites of the electrode surface. This makes it necessary to look for the new approaches towards the development of effective anodic catalysts providing the sufficiently high rate and oxidation depth of ethanol. There are certain advantages in using alkaline electrolytes, as their relatively low corrosive activity opens the possibility of using nickel, iron, cobalt, and their oxides. Some of

†Corresponding author. Tel.: +98-21-22853551
E-mail address: jafarian@kntu.ac.ir

the data on ethanol oxidation in an alkaline electrolyte on platinum are presented in work,[20] in which the authors observed the strong passivation of platinum and came to the conclusion about the necessity of developing a more acceptable catalyst than platinum. In further works,[21,22] ethanol oxidation was studied in 1 M KOH on titanium promoted by RuO_2/Ni system and glassy carbon coated by RuNi nanoparticles. The activity of these catalysts was low, and the starting potential of alcohol oxidation was close to 0.9 V vs. the reversible hydrogen electrode (RHE). Therefore, the development of a catalyst that oxidizes ethanol is of high interest. Electrochemical oxidation of ethanol at nickel electrode was studied by Park *et al.*[23] in 1 m KOH solution containing 0.2 M ethanol using electrochemical impedance spectroscopy. The results suggested that the β-$Ni(OH)_2$/β-NiOOH redox couple is acting as an effective electron transfer mediator for ethanol oxidation.

The purpose of the present work is to study the kinetic of oxidation reaction of ethanol on a nickel modified NiOOH electrode in room temperature in basic solution.

2. Methods and Materials

Sodium hydroxide and ethanol used in this work were Merck products of analytical grade and were used without further purifications. Doubly distilled water was used throughout.

Electrochemical studies were carried out in a conventional three electrode cell powered by an electrochemical system comprising of EG&G model 273 potentiostat/galvanostat. The system is run by a PC through M270 commercial softwares via a GPIB interface. A dual Ag/AgCl-Sat'd KCl, a Pt wire and a nickel disk electrode were used as the reference, counter and working electrodes, respectively. All studies were carried out at 298 ± 2 K.

The nickel disk electrode was polished with 0.05 mm alumina powder on a polishing micro-cloth and rinsed thoroughly with doubly distilled water prior to modification. Cyclic voltammetry from 0-0.6 V vs. Ag/AgCl with 50 cycles was used for electrode surface modification and activation.[24]

3. Results and discussion

Fig. 1 presents consecutive cyclic voltammograms

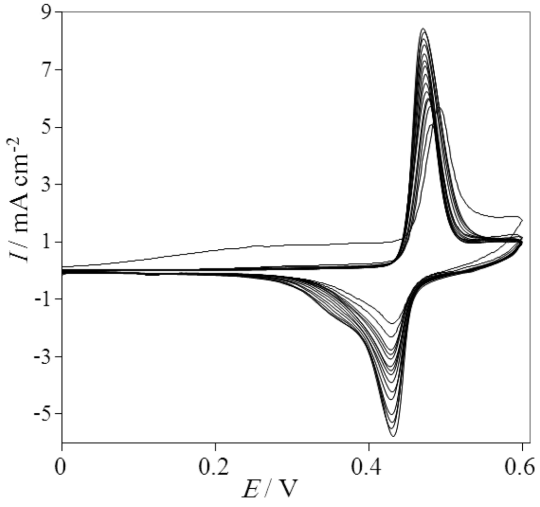

Fig. 1. Consecutive cyclic voltammogram of Ni oxidation in 1M NaOH comprised of different sweep number (1, 2, 3, 4, 5, 6, 10, 15, 20, 25, 30, 35, 40, 45, 50) at a scan rate of 100 mV s^{-1}.

(CV) of a nickel electrode in 1 M NaOH solution recorded at a potential sweep rate of 100 mV s^{-1}. In the first sweep a pair of redox peaks appear at 492 and 429 mV vs. Ag/AgCl that are assigned to the Ni^{2+}/Ni^{3+} redox couple according to:

$$Ni(OH)2 + OH^- \leftrightarrow NiOOH + H_2O + e^-$$

In the subsequent cycles both the anodic and cathodic peaks shift negatively and stablize pointing to higher energies (potential) required for nucleation of NiOOH in the first cycle. The enhanced base line current of the first cycle is associated with the oxidation of Ni to Ni^{2+}.

The current grows with the number of potential scans indicating the progressive enrichment of the accessible electroactive species Ni^{2+} and Ni^{3+}on or near the surface and stabilized after 50 cycles. After prolong cycling, the redox peak potential are stabilized at 472 and 427 mV vs. Ag/AgCl and a shoulder develops on cathodic peak at around 350 mV. The changes of the peaks position and also creation of a new reduction peak are likely due to the changes[25] in the crystal structures of the nickel hydroxide and the nickel oxyhydroxide constituents of the electrochemically formed surface film. It has been reported[26,27] that at the initial stages of electro-oxidation α-$Ni(OH)_2$ forms and is further slowly converted to the β-$Ni(OH)_2$ form.[28,29]

Fig. 2(a) presents typical CVs of a Ni electrode in

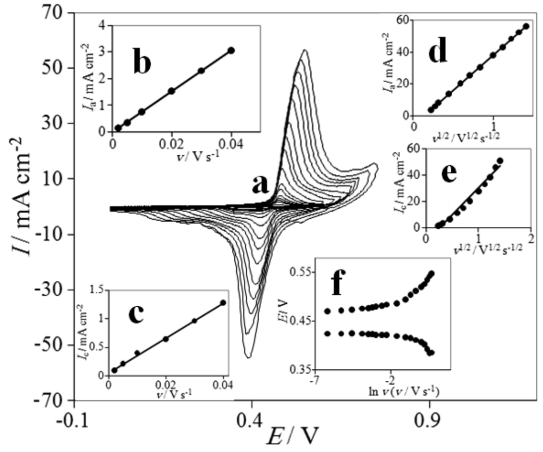

Fig. 2. (a) Typical cyclic voltammograms of a Ni electrode in 1 M NaOH in the potential sweep rates of 2, 5, 10, 20, 50, 100, 200, 350, 500, 700, 1000, 1250, 1500, 1750, 2000 mV s^{-1}, (b) the dependency of anodic and (c)cathodic peak currents to the sweep rate at lower values (2-40 mV s^{-1}). (d) The proportionality of anodic and (e) cathodic peak currents to the square roots of sweep rate at higher values (50-2000 mV s^{-1}). (f) Plot of E_p *vs.* ln *v* for cyclic voltammograms depicted in panel (a) for anodic peaks (1) and cathodic peaks (2).

1 M NaOH solution at various potential sweep rates of 2-2000 mV s^{-1}. The peak current is proportional to sweep rates in the range of 2-40 mV s^{-1}, Fig. 2(b) and (c), pointing to the electrochemical activity of the surface redox couple.[30] From the slope of these lines and using:

$$I_p = \left(\frac{n^2F^2}{4RT}\right)\nu A\Gamma^* \quad (1)$$

where Γ^* is the surface coverage of the redox species and *v* being the potential sweep rate and taking average of both cathodic and anodic results, Γ^* values of around 5.7×10^{-8} mol cm^{-2} has been derived that correspond to the presence of around 60 monolayers of surface species. In the higher potential sweep rates this dependency is of square root form, Figs. 2(d) and 2(e).

Laviron[31] derived general expressions for the cyclic voltammetric response for the case of surface-confined electro-reactive species at small concentrations. The following simplified relations were proposed:

$$E_{pa} = E^0 + A\,ln\left[\frac{1-\alpha}{m}\right] \quad (2)$$

$$E_{pc} = E^0 + B\,ln\left[\frac{\alpha}{m}\right] \quad (3)$$

$$ln\,k_s = \alpha\,ln(1-\alpha) + (1-\alpha)\,ln\alpha - ln\left(\frac{RT}{nF\nu}\right) - \frac{\alpha(1-\alpha)nF\Delta E_p}{RT} \quad (4)$$

where $A = RT/(1-\alpha)nF$, $B = RT/\alpha nF$, $m = (RT/F)(k_s/n\nu)$, E_{pa} and E_{pc} are anodic and cathodic peak potential respectively, and ν the potential sweep rate, respectively. From these expressions, α can be determined by measuring the variation of the peak potential with respect to the potential sweep rate, and k_s can be determined for electron transfer between the electrode and surface modified layer by measuring the E_p values. Fig. 2(f), shows the plot of E_p with respect to the ln ν from cyclic voltammograms recorded for Ni electrode in 1 M NaOH solution at potential sweep rates of 2-2000 mV s^{-1} for anodic (1) and cathodic (2) peaks. It can be observed that for potential sweep rates of 200-1000 mV s^{-1} the values of E_p are proportional to the logarithm of the potential sweep rate indicated by Laviron. Using the plot and Eq. (4), the values of α and k_s were determined as 0.43 and 0.26 s^{-1}, respectively.

Fig. 3 shows cyclic voltammograms of Ni electrode in 1 M NaOH solution in the absence (1) and presence (2) at of various concentrations of ethanol ranging from 0.1 to 1 M and at a potential sweep rate of 10 mV s^{-1}. At Ni electrode, oxidation of ethanol appeared as a typical electrocatalytic response. The anodic charge increased with respect to that observed for the modified surface in the absence of ethanol and it was followed by decrease in the cathodic charge upon increasing the concentration of ethanol in solution. In the presence of 0.7 M ethanol with the potential sweep rate of 10 mV s^{-1}, the ratio of anodic to cathodic charge in the presence of ethanol was 98.5/1.5 while in its absence it was 56/44. Charge is obtained by integrating the anodic and cathodic peaks after the background correction.

The anodic current in the positive sweep was proportional to the bulk concentration of ethanol and any increase in the concentration of ethanol caused an almost proportional linear enhancement of the anodic current (Fig. 3(c)).

The decreased cathodic current that ensued the oxidation process in the reverse cycle indicated that the rate determining step certainly involves ethanol and

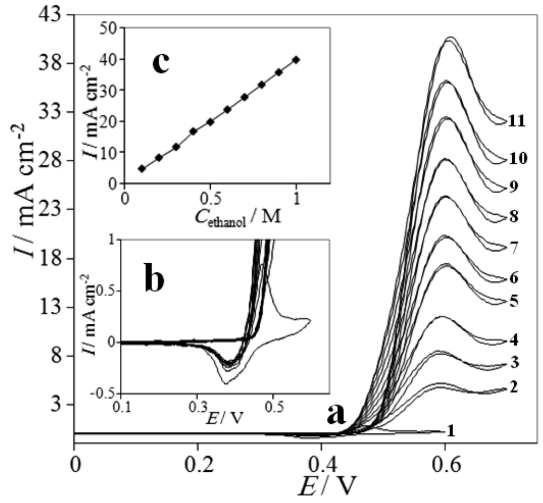

Fig. 3. (a) Cyclic voltammograms of the Ni electrode in 1 M NaOH solution in the absence (1) and the presence (2) 0.1 M; (3) 0.2 M; (4) 0.3 M; (5) 0.4 M; (6); 0.5 M; (7) 0.6 M; (8) 0.7 M; (9) 0.8 M; (10) 0.9 M; (11) 1 M of ethanol in the solution. Potential sweep rate was 10 mV s^{-1}. (b) Initial potential of ethanol oxidation. (c) Dependency of the anodic peak current on the concentration of ethanol in solution.

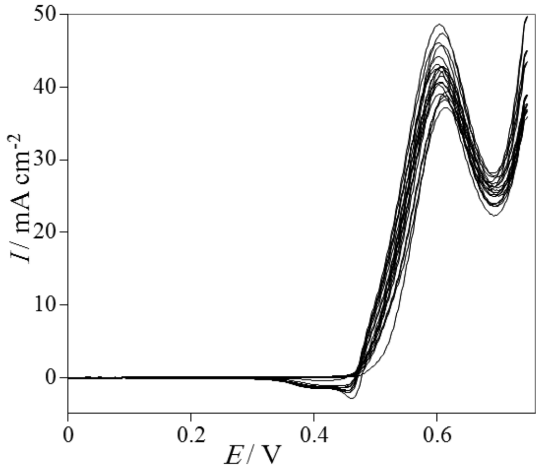

Fig. 4. Repeated cyclic voltammograms of 0.5 M ethanol oxidation on Ni electrode at 50 mV s^{-1}, cycle number: 1, 5, 10, 20, 50, 100, 150, 200, 250, 300.

that it was incapable of reducing the entire high valent nickel species formed in the oxidation cycle.

The electrocatalytic oxidation of ethanol occurs not only in the anodic but also continues in the initial stage of the cathodic half cycle. Ethanol molecules adsorbed on the Ni^{2+} species are oxidized at higher potentials parallel to the oxidation of Ni^{2+} to Ni^{3+} species. The later process has the consequence of decreasing the number of sites for ethanol adsorption that along with the poisoning effect of the products or intermediates of the reaction tends to decrease the overall rate of ethanol oxidation. Thus, the anodic current passes through a maximum as the potential is anodically swept. In the reverse half cycle, the oxidation continues and its corresponding current goes through the maximum due to the regeneration of Ni(II) species that are active sites for the adsorption of ethanol as a result of removal of adsorbed intermediates and products. Surely, the rate of ethanol oxidation as signified by the anodic current in the cathodic half cycle drops as the unfavorable cathodic potentials are approached.

Fig. 4 shows the cyclic voltammograms of Ni electrode in 1 M NaOH in presence of 0.5 M ethanol at a scan rate of 50 mV s^{-1} for 300 cycles. It is observed that the current density of electrooxidation of ethanol is almost constant in 300 cycles due to the stability of electrocatalyst in this cycle number and indicating that ethanol reacted with the surface and no poisoning effect on the surface was observed.

Cyclic voltammograms of Ni in the presence of 0.5 M ethanol at various potential sweep rates and the proportionality of anodic peak currents to the square root of sweep rates in a range of 2 to 500 mV s^{-1} are illustrated in Fig. 5(a), (b), respectively. The cathodic peak was not observed in low scan rates, but appeared upon increasing the sweep rate. The phenomenon indicates that the electrooxidation of nickel species to higher valence state is much faster than the catalytic oxidation of ethanol. This reveals that the oxidation of ethanol on Ni may belong to a slow process. At higher scan rates a new oxidation peak observed for ethanol oxidation at a potential much more positive than that of the oxidation of $Ni(OH)_2$ potential. Meanwhile, the anodic peak currents that are linearly proportional to the square root of scan rate (Fig. 5(b)) suggest that the overall oxidation of ethanol at this electrode is controlled by the diffusion of ethanol from solution to the surface redox sites. From the slope of the straight line the diffusion coefficient of ethanol was obtained as 2×10^{-7} cm^2 s^{-1}. Moreover, a plot of the scan rate-normalized current ($I/v^{1/2}$) with respect to scan rate (Fig. 5(c)) exhibited a typical shape of an electrochemical–chemical (EC) catalytic process.[32] The value of electron transfer coefficient for the reaction which is totally irreversible-diffusion controlled can be

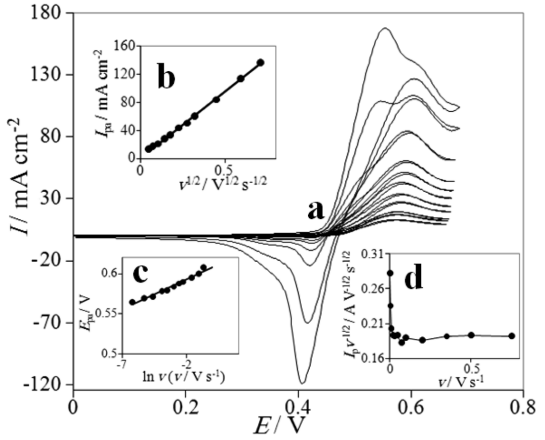

Fig. 5. (a) Typical cyclic voltammograms of the Ni in 1 M NaOH in the presence of 0.5 M ethanol at various potential sweep rates of 2, 5, 10, 20, 30, 40, 50, 75, 100, 200, 350 and 500 mV s^{-1}. (b) Dependence of anodic peak current during the forward sweep on the square roots of sweep rate. (c) The anodic current function ($I/i^{1/2}$) vs. potential sweep rate *v*. (d) Dependence of the peak potential on ln *v* for the oxidation of ethanol at GC/Ni electrode.

obtained from the following equation[33]:

$$E_P = \left(\frac{RT}{n\alpha F}\right) lnv + \text{constant} \quad (5)$$

Using the dependency of anodic peak potential on the natural logarithm of the potential sweep rate (Fig. 5(d)), the value of electron transfer coefficient was obtained as 0.87.

High current density was observed in presence of ethanol in comparison to the $Ni(OH)_2$. Also a new oxidation peak was obtained for ethanol oxidation at a potential much more positive than that of the oxidation of $Ni(OH)_2$ potential. According to these data it can be assume that partly of the current is due to ethanol oxidation by NiOOH due to the disappearance of the NiOOH reduction peak in the negative sweep, Eq. (7) & (8), and partly of the current is due to ethanol oxidation on the surface of oxide or within (inside) the oxide layer, Eq. (9) & (10).

The redox transition of nickel species present in the film is:

$$Ni(II) \xleftrightarrow{v_1} NI(III) + e^- \quad (6)$$

and ethanol is oxidized on the modified surface via the following reaction:

$$Ni^{3+} + \text{ethanol} \xrightarrow{v_2} Ni^{2+} + \text{intermediate} \quad (7)$$

$$Ni^{3+} + \text{intermediate} \xrightarrow{v_3} Ni^{2+} + \text{products} \quad (8)$$

where Ni^{3+} sites are regenerated by the power source and on the Ni^{3+} oxide surface by direct electro-oxidation[34,35]

$$Ni^{3+} - \text{ethanol} \xrightarrow{v_4} Ni^{3+} - \text{intermediate} + 3 \quad (9)$$

$$Ni^{3+} - \text{intermediate} \xrightarrow{v_5} Ni^{3+} - \text{products} + e \quad (10)$$

Eqs. (7) & (8) is according to Fleischmann mechanism and in Eqs. (9) & (10), Ni^{3+} used as active surface for ethanol oxidation. Observation of a new oxidation peak for ethanol oxidation at a potential much more positive than that of the oxidation of $Ni(OH)_2$ potential is according to Eqs. (9) & (10). According to above equation the Faradaic current density can be written as:

$$I_F = (v_1 + v_4 + v_5)F \quad (11)$$

Setting the working electrode potentials to desired values, the measurement of the catalytic rate constant as well as the diffusion coefficient of ethanol was performed under chronoamperometric regime. Fig. 6(a) shows double steps choronoamperograms for the Ni in the absence (1) and presence (2-6) of ethanol over a concentration range of 0.1 to 0.9 M with an applied potential steps of 620 and 300 mV, respectively. Plotting of net current with respect to the mines reverse

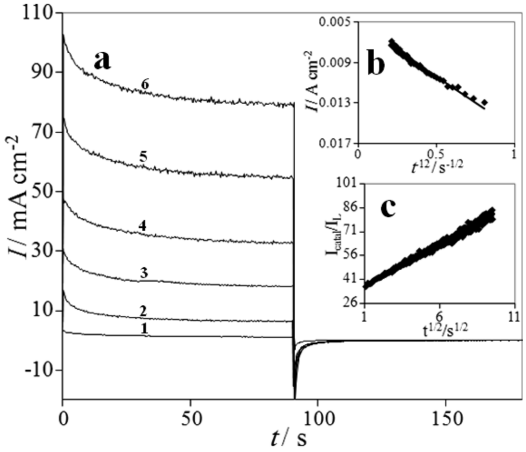

Fig. 6. (a) Double steps chronoamperograms of Ni electrode in 1 M NaOH solution with different concentrations of ethanol of: (1) 0 M, (2) 0.1 M, (3) 0.3 M, (4) 0.5 M, (5) 0.7 M and (6) 0.9 M. Potential steps were 620 mV and 300 mV, respectively. (b) Dependency of transient current on $t^{-1/2}$. (c) Dependence of I_{catal}/I_L on $t^{1/2}$ derived from the data of chronoamperograms of 1 and 6 in panel (a).

square roots of time, after removing the background current presents a linear dependency (Fig. 6(b)). The dominance of a diffusion-controlled process is evident. Using the slope of this line in Cottrell equation[30]:

$$I = nFAD^{1/2}C^*\pi^{-1/2}t^{-1/2} \quad (12)$$

the diffusion coefficient of ethanol has been obtained to be 1×10^{-7} cm^2 s^{-1} which is in good agreement with value with the value obtained by cyclic voltammetry. The current is also negligible when potential is stepped down to 320 mV, indicating the irreversibility of ethanol oxidation process.

Choronoamperometry can also be used for the evaluation of the catalytic rate constant[36]

$$\frac{I_{cat}}{I_L} = \gamma^{1/2}\left[\pi^{1/2}erf(\gamma^{1/2}) + \frac{\exp(-\gamma)}{\gamma^{1/2}}\right] \quad (13)$$

where I_{cat} and I_L are the currents of the Ni in the presence and absence of ethanol and $\gamma = kC^*t$ is the argument of the error function. k is the catalytic rate constant, C^* is bulk concentration of ethanol and t is elapsed time (s). In the cases where $\gamma > 1.5$, $erf(\gamma^{1/2})$ is almost equal to unity and the above equation simplifies to:

$$\frac{I_{cat}}{I_L} = \gamma^{1/2}\pi^{1/2} = \pi^{1/2}(kC^*t)^{1/2} \quad (14)$$

From the slope of the I_{cat}/I_L vs. $t^{1/2}$ plot, presented in Fig. 5(c) the mean value of k for the concentration range of 0.1 M to 0.9 M of ethanol was obtained as 9.64×10^3 cm^3 mol^{-1} s^{-1}.

In comparison with recently published work for ethanol electrocatalytic oxidation on Pt, Pd, Au and its alloys,[37-39] higher oxidation current density and catalytic activity was obtained for nickel modified NiOOH electrode.

4. Conclusions

The nickel oxide film was formed electrochemically on nickel electrode in a regime of cyclic voltammetry and tested for electrooxidation of ethanol in alkaline media. The modified electrode showed electrocatalytic activity for the oxidation of ethanol at around 600 mV vs. Ag/AgCl. The Ni modified nickel oxyhydroxide electrode exhibited large response current for oxidation of ethanol. A kinetic model was developed and using the methods of cyclic voltammetry, chorono-amperometry, the kinetic parameters such as transfer coefficient (α), the catalytic reaction rate constants (k), and the diffusion coefficient of ethanol in the bulk of solution were determined.

References

1. H. Uchida, Y. Mizuno and M. Watanabe, *J. Electrochem. Soc.* **149**, A682 (2002).
2. W. C. Choi, J. D. Kim and S. I. Woo, *Catal. Today* **74**, 235 (2002).
3. Z. B. Wang, G. P. Yin and P. F. Shi, *Carbon* **44**, 133 (2006).
4. C. Lamy, E. M. Belgsir and J.-M. Leger, *J. Appl. Electrochem.* **31**, 799 (2001).
5. E. V. Spinace, A. O. Neto and M. Linardi, *J. Power Sources* **124**, 426 (2003).
6. W. J. Zhou, S.Q. Song, W. Z. Li, Z. H. Zhou, G. Q. Sun, Q. Xin, S. Douvartzides and P. Tsiakaras, *J. Power Sources* 140, 50 (2005).
7. Z. B. Wang, G. P. Yin, J. Zhang, Y. C. Sun and P. F. Shi, *J. Power Sources* **160**, 37 (2006).
8. G. A. Camara, R. B. de Lima and T. Iwasita, *Electrochem. Commun.* **6**, 812 (2004).
9. C. Lamy, S. Rousseau, E. M. Belgsir, C. Coutanceau, and J.-M. Leger, *Electrochim. Acta* **49**, 3901 (2004).
10. A. O. Neto, M. J. Giz, J. Perez, E. A. Ticianelli and E. R. Gonzalez, *J. Electrochem. Soc.* **149**, A272 (2002).
11. J. M. Leger, S. Rousseau, C. Coutanceau, F. Hahn and C. Lamy, *Electrochim. Acta* **50**, 5118 (2005).
12. J. P. I. Souza, S. L. Queiroz, K. Bergamaski, E. R. Gonzalez and F. C. Nart, *J. Phys. Chem.* B **106**, 9825 (2002).
13. T. Iwasita and E. Pastor, *Electrochim. Acta* **39**, 531 (1994).
14. T. Iwasita, R. Dalbeck, E. Pastor and X. Xia, *Electrochim. Acta* **39**, 1817 (1994).
15. H. Hitmi, E. M. Belgsir, J.-M. Leger, C. Lamy and R. O. Lezna, *Electrochim. Acta* 39, 407 (1994).
16. J. Shin, W. J. Tornquist, C. Korzeniewski and C. S. Hoaglund, *Surf. Sci.* **364**, 122 (1996).
17. X. H. Xia, H. D. Liess and T. Iwasita, *J. Electroanal. Chem.* 437, 233 (1997).
18. J. F. E. Gootzen, A. H. Wonders, A. P. Cox, W. Visscher and J. A. R. Van Veen, *J. Mol. Catal. A: Chem.* **127**, 113 (1997).
19. R. Ianniello, V. M. Schmidt, J. L. Rodriguez and E. Pastor, *J. Electroanal. Chem.* 471, 167 (1999).
20. S.-M. Park, N. Chen and N. Doddapaneni, *J. Electrochem. Soc.* **142**, 40 (1995).
21. J.-W. Kim and S.-M. Park, *J. Electrochem. Soc.* **146**, 1075 (1999).
22. J.-W. Kim and S.-M. Park, *J. Electrochem. Solid State Lett.* **3**, 385 (2000).

23. J. W. Kim, S. M. Park, *J. Korean Electrochem. Soc.* **8**, 117 (2005).
24. M. Jafarian, F. Forouzandeh, I. Danaee, F. Gobal and M. G. Mahjani, *J. Solid State Electrochem.* **13**, 1171 (2009).
25. A. A. El-Shafei, *J. Electroanal. Chem.* **471**, 89 (1999).
26. I. Danaee and M. Jafarian, A. Mirzapoor, F. Gobal, M.G. Mahjani, *Electrochim. Acta* **55**, 2093 (2010).
27. F. Hahn, B. Beden, M. J. Croissant and C. Lamy, *Electrochim. Acta* **31**, 335 (1986).
28. J. Desilvestro, D. A. Corrigan and M. J. Weaver, *J. Electrochem. Soc.* **135**, 885 (1988).
29. I. Danaee, M. Jafarian, F. Forouzandeh, F. Gobal and M. G. Mahjani, *Electrochim. Acta* (2008) **53**, 6602.
30. A. J. Bard and L. R. Faulkner, Electrochemical Methods, fundamentals and applications, Wiley, New York, 2001, p. 591.
31. E. Laviron, *J. Electroanal. Chem.* **101**, 19 (1979).
32. R. S. Nicholson and I. Shain, *Anal. Chem.* **36**, 706 (1964).
33. J. A. Harrison and Z. A. Khan, *J. Electroanal. Chem.* **28**, 131 (1970).
34. I. Danaee, M. Jafarian, F. Forouzandeh, F. Gobal and M. G. Mahjani, *Int. J. Hydrogen Energy* **34**, 859 (2009).
35. I. Danaee, M. Jafarian, F. Forouzandeh, F. Gobal and M. G. Mahjani, *J. Phys. Chem. B* **112**, 15933 (2008).
36. I. Danaee, M. Jafarian, F. Forouzandeh, F. Gobal and M. G. Mahjani, *Int. J. Hydrogen Energy* **33**, 4367 (2008).
37. C. Li, Y. Su, X. Lv, H. Shi, X. Yang and Y. Wang, *Mater. Lett.* **69**, 92 (2012).
38. X. Han, D. Wang, D. Liu, J. Huang and T. You, *J. Colloid Interface Sci.* **367**, 342 (2012).
39. G. Hu, F. Nitze, H. R. Barzegar, T. Sharifi, A. Mikołajczuk, C.-Wai Tai, A. Borodzinski and T. Wagberg, *J. Power Sources* **209**, 236 (2012).